Biosensors and Bioelectronics 58 (2014) 214–218

Contents lists available at ScienceDirect

Biosensors and Bioelectronics

journal homepage: www.elsevier.com/locate/bios

Coupling exonuclease III with DNA metallization for amplified detection of biothiols at picomolar concentration

Zhaowei Chen, Li Zhou, Andong Zhao, Zhijun Zhang, Zhenzhen Wang, Youhui Lin, Jinsong Ren*, Xiaogang Qu

State Key Laboratory of Rare Earth Resource Utilization and Laboratory of Chemical Biology, Changchun Institute of Applied Chemistry, Graduate School of the Chinese Academy of Sciences, Chinese Academy of Sciences, Changchun, Jilin 130022, China

ARTICLE INFO

Article history:
Received 5 December 2013
Received in revised form
14 February 2014
Accepted 18 February 2014
Available online 6 March 2014

Keywords:
DNA
Metallization
Exonuclease III
Biothiols
Amplified detection

ABSTRACT

For early diagnosis of diseases, the need of ultralow detection limit is an ongoing quest. In this work, by taking the uniqueness of Exonuclease III and DNA metallization, we demonstrate a facile turn-on fluorescent method for amplified detection of biothiols at picomolar concentration. This method relies on the amplification process achieved by the recycling of biothiols retrieved target DNA from silver depositions and the specific interactions between quadruplex and NMM. This method is simple in design, economic in operation and exhibits ultralow detection limit and excellent selectivity toward thiol-containing biomolecules among amino acids found in proteins and in serum samples. More importantly, the detection and discrimination process can be seen by the naked eye with the aid of an UV transilluminator. Therefore, this new concept may offer a potential approach for practical applications as an efficient biosensor for early detection of diseases.

1. Introduction

Biothiols such as cysteine (Cys), homocysteine (Hcy) and glutathione (Gsh) play crucial biological roles in human body such as crosslinking proteins, maintaining intracellular redox activities (Stryer, 1995; Yi et al., 2009). Abnormal level of these thiol contained biomolecules in biological fluids is associated with many risk diseases such as cancer, heart disease and AIDS (Herzenberg et al., 1997; Jacobsen, 1998). Accordingly, efficient measurements of mercapto-amino acids, especially under normal physiological conditions, are highly desirable. A variety of methods for detecting biothiols, such as fluorescent assays, (Tanaka et al., 2004; Zhang et al., 2007) high-performance liquid chromatography techniques, (Lu et al., 2007; Tcherkas and Denisenko, 2001) and electrochemical voltammetry (Hignett et al., 2001; Zen et al., 2001) have been developed. However, most of them require complicated instruments, involve cumbersome laboratory procedures and are low throughput, which limits the scope of their practical applications. Thus, the development of rapid, cost-effective, sensitive and specific methods for biothiol detection is vitally important.

DNA has been an extremely favorable tool in establishing biosensors not only for proteins but also low molecular weight substrate (such as ATP, biothiols, etc.) (Wang et al., 2006, Song et al., 2010, Xiao et al., 2005). For example, Lee et al. (2008) developed a colorimetric method for cysteine detection by using DNA functionalized gold nanoparticle probes that contain strategically placed thymidine–thymidine mismatches complexed with Hg^{2+}. Recently, our group has proposed a biothiol detection approach by utilizing silver metallized DNA as probe (Lin et al., 2011). Although promising, for early diagnosis of diseases, the need of ultralow detection is an ongoing quest (Wulfkuhle et al., 2003) and especially, the search for a thiol detection platform with limit below nanomolar still remains a big challenge.

Recently, Exonuclease III (Exo III) has been reported as an efficient biocatalyst for amplified detection of DNAs, proteins, or other small molecules with ultralow detection limit (Freeman et al., 2011; Zuo et al., 2010; Wang et al., 2006; Song et al., 2010; Xiao et al., 2005; Zhao et al., 2003; Liu and Lu, 2003, 2007; Ma et al., 2013; Duan et al., 2013; Wei et al., 2012). Exo III could selectively digest the 3'-end of nucleic acid strands in duplex DNAs, thus enabling the selective cleavage of one of the strands in double-stranded DNA structures (Zhao et al., 2011). This function was used to develop different Exo III-based amplified detection platforms that involved the biocatalytic recycling of the target DNA by Exo III (Peng et al., 2012; Liu et al., 2012; Ju et al., 2012). Nonetheless, up to this stage, Exo III-based amplified platforms that recycle DNA recovered from inorganic depositions at present

* Correspondence to: Laboratory of Chemical Biology, Division of Biological Inorganic Chemistry, State Key Laboratory of Rare Earth Resource Utilization, Changchun Institute of Applied Chemistry, Chinese Academy of Sciences, Changchun, Jilin 130022, China. Fax: +86 431 85262526.
E-mail address: jren@ciac.ac.cn (J. Ren).

http://dx.doi.org/10.1016/j.bios.2014.02.078
0956-5663

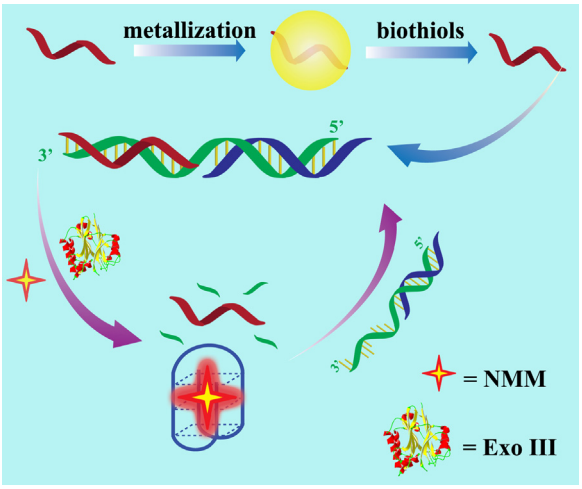

Scheme 1. Schematic illustration of the strategy for amplified detection of biothiols by coupling Exo III and DNA metallization.

are unknown. As a promising deposition technology, DNA metallization, where metal structures deposit following DNA contour, provides a wide range of potential applications in electronics, biosensing, pattern transfer and dynamic nanomaterials (Keren et al., 2002, 2004; Braun et al., 1998; Jin et al., 2013). For example, silver metallization could destroy the recognition properties of the DNA, thus preventing the subsequent biological processes (Keren et al., 2004; Lin et al., 2011). Meanwhile, silver nanoparticles could be mildly etched by thiols, which had been used to fine tune the shape and morphology of metal nanostructures (Cho et al., 2009; Quaroni and Chumanov, 1999). Therefore, bitothiols could be expected to retrieve DNA from biologically blocked state in silver depositions.

Inspired by those phenomena, herein, for the first time, by taking advantages of the uniqueness of Exo III and DNA metallization, we developed a highly sensitive platform for analyzing biothiols at picomolar concentration (Scheme 1). After silver metallization, the target DNA (**T**) is biologically blocked and could not hybridize with its complementary sequence parts (**Tc**) in the probe DNA (**P/G4**), thus avoiding digestion by Exo III. Upon the addition of biothiols, the silver metalized **T** could be readily released due to the etching interaction between thiol and silver. When the duplex probe is challenged with the extracted **T** from silver depositions, the hybridization leads to a blunt 3'-terminus, which can be catalyzed by Exo III. Then, the extracted **T** and a quadruplex-forming oligomer (**G4**) can be released. The intriguing interaction between the activated quadruplex and its specific ligand, N-methyl mesoporphyrin IX (NMM), brings about a great fluorescence enhancement for signal readout (Hu et al., 2010). During the catalysis step, the retrieved **T** is ready to bind to another probe **P/G4** to initiate a new cycle, generating a concomitant increase in fluorescence. The design of each DNA sequence was described in the experiment sections.

2. Experimental section

2.1. Reagents

The DNA sequences used in the study were as follows:

T: 5'-CTGTTGTGACTCGTCGCAATAAC-3',
Tc: 5'-GCGACGAGTCACAACAG-3',
G4: 5'-CTCTTCGAGGGTTTTGGGTTTTGGGTTTTGGGAGCTA-3',
P: 5'-AAAACCCAAAACCCAAAACCCGCGACGAGTCACAACAG-3',

The **G4** DNA was designed partially complementary to **P** DNA with two bases mismatched at 5'-terminus. When the **P/G4** probe was challenged with perfectly matched target DNA, ssDNA at 5' end of the probe hybridized with the perfectly matched target DNA. Then the mismatched part of **G4** would be displaced by the target DNA. Degraded by Exo III, the probe that hybridized with target DNA would release target DNA. Then the mismatched part of **G4** DNA which was displaced by target DNA previously, would hybridize with **P/G4** DNA again to make sure the digestion continue.

The DNA oligomer was synthesized by Shanghai Sangon Biological Engineering Technology & Services (Shanghai, China). NMM was purchased from Porphyrin Products (Logan, UT), and its concentration was measured by using absorbance spectroscopy on a JASCO V-550 and found to be λ=379 nm, assuming an extinction coefficient of $1.45\times10^5\ M^{-1}\ cm^{-1}$. Silver nitrate ($AgNO_3$) and sodium borohydride ($NaBH_4$) were purchased from Alfa Aesar. Other chemicals including amino acids and biothiols were purchased from Sigma-Aldrich and used without further purification. All the water used to prepare buffer solutions was obtained by using a Milli-Q water system. All measurements were performed in Mg–K buffer (10 mM Tris–HCl, 75 mM KCl, 10 mM $MgCl_2$, pH 8.0). The fluorescence spectra were recorded using a JASCO FP6500 spectrophotometer (JASCO International Co. Ltd., Tokyo, Japan). The concentration of DNA was determined using a JASCO V-550 UV/Vis spectrophotometer, equipped with a temperature-controlled cuvette holder. TEM images were recorded using a FEI TECNAI G2 20 high-resolution transmission electron microscope operating at 200 kV. CD spectra were determined using a Jasco 810 (Jasco International Co., Ltd., Tokyo, Japan)

2.2. Synthesis of DNA–silver nanohybrids

The DNA–silver nanohybrids were synthesized by reduction of $AgNO_3$ with $NaBH_4$. Briefly, DNA was mixed excess $AgNO_3$ (50:1 Ag^+/**T** molar ratio). After 30 min of incubation, freshly prepared $NaBH_4$ solution (Ag^+ and $NaBH_4$ were mixed in a 1:5 molar ratio) was dropped into the above aqueous solution under vigorous stirring. After mixing, the resulting yellow colloidal silver solution was stirred for another 30 min.

2.3. Fluorescence assay for biothiols detection

The fluorescence intensity of all samples was analyzed via a time base scan. The solutions were excited at 399 nm, and emission spectra were collected from 550 to 750 nm. Slit widths for the excitation and emission were set at 10 and 10 nm, respectively. All measurements were performed in Mg–K buffer (10 mM Tris–HCl, 75 mM KCl, 10 mM $MgCl_2$, pH 8.0). In a typical procedure, silver metalized **T** was mixed with different concentrations of biothiols or other analytes. The mixture was equilibrated for 0.5 h at 37 °C. Then, 40 U Exo III and **P**/**G4** were added and the solution was incubated in 37 °C for 0.5 h. Finally, NMM was added and equilibrated for 5 min before spectral measurements. The final concentrations of **T**, **P**/**G4** and NMM were 20 nM, 0.5 μM and 1 μM, respectively. For visual detection of biothiols Exo III catalyzed reactions were kept for 2 h at 37 °C; the final concentrations of **T**, **P**/**G4** and NMM were 200 nM, 1.5 μM and 3 μM, respectively. Photographs of the solutions were taken using a UV transilluminator.

2.4. Preparation of real samples

Fresh human blood samples were collected in tubes containing EDTA, and centrifuged at 5000 rpm for 20 min. The supernatant solution, which contains proteins and amino acids, was used as the

source of plasma. Since most of the thiol compounds in plasma were linked to other thiols and proteins by disulfide bonds, it was necessary to reduce disulfide bonds before analysis and the following procedure according to literatures was carried out. Firstly, 40 μl of HCl (0.2 M) and 20 μl of PPh_3 (400 mM in H_2O–CH_3CN 20:80 v/v and 2.0 M HCl) were added to 500 μl of plasma and incubated for 15 min at room temperature to hydrolyze the disulfide bonds. After that, 500 μl of CH_3CN was mixed with 500 μl of hydrolyzed plasma to precipitate plasma proteins followed by centrifugation at 3000*g* for 20 min twice. The supernate containing thiol compounds was collected for further analysis. Since the thiols content of plasma is beyond the dynamic range of the proposed method, the plasma sample has been appropriately diluted with Tris–HCl buffer before measurement. For recovery studies known concentrations of Cys were added to plasma samples and the total thiol concentrations were then determined.

3. Results and discussion

3.1. Synthesis and characterization of DNA–silver hybrids

To demonstrate the feasibility of our protocol, several key experiments have been performed. Firstly, in order to prove that silver deposition can disrupt the hybridization between **T** and **Tc** in the probe DNA, the fluorescence response of a double strand intercalating dye GeneFinder (GF) which exhibits intense fluorescence upon intercalating double-strand was measured. Silver deposition in different molar ratios of Ag^+ to **T** were produced by reduction of Ag^+ bound to the DNA with $NaBH_4$. As shown in Fig. S1 (in the Supplementary information), the fluorescence intensity of GF decreased gradually with increasing Ag^+/**T** molar ratio in the presence of sliver deposited **T** and **Tc**. The fluorescence signal of the mixture is close to the emission intensity of the mixture of GF and **Tc** at the molar ratio of Ag^+ to DNA equal to 50:1. Then, the resulting DNA–silver hybrid solutions were studied by UV–vis absorption (Fig. 1a). The UV–vis absorption spectra of the silver metalized **T** exhibited the DNA absorption peak at 260 nm and the surface plasmon response band centered at 430 nm. Transmission electron microscopy (TEM) image (Fig. 1b) and the corresponding size distribution histogram (Fig. S2, in the Supplementary information) revealed that the resulting silver deposited DNA nanoparticles have an average size of 3.4 nm. After etching with biothiols, the solution exhibited a new peak around 360 nm (Fig. 1a) which could be attributed to the formation of Ag–S–R compounds during the etching reaction (Cho et al., 2009). Correspondingly, the solution color changed from yellow to tansparent upon the addition of biothiols (Fig. 1a, inset ii and iii). Moreover, DNA melting test clearly indicated that biothiols can effectively recover DNA from silver depositions to induce duplex formation between the extracted target **T** and **Tc** (Fig. 1c), which is a prerequisite for further Exo III based recycling system. Next,

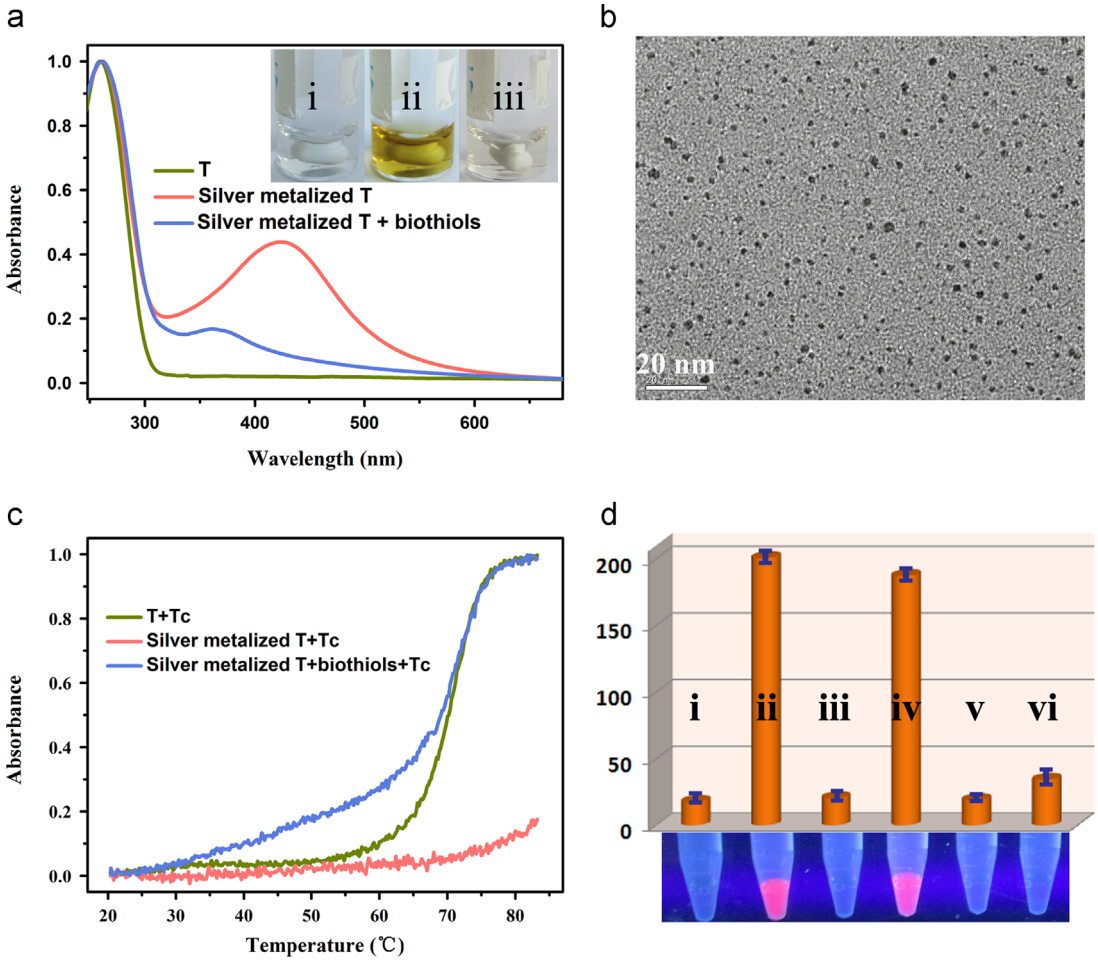

Fig. 1. (a) UV–vis absorbance spectra of solutions containing **T**, silver metalized **T** and silver metalized **T**+ +biothiols and inset shows corresponding photographs i, ii, and iii, respectively. (b) TEM image of DNA template silver metallization. (c) Thermal melting profiles of solutions containing **T**+ +**Tc**, silver metalized **T**+ +**Tc** and biothiols extracted **T**+**Tc**. (d) Fluorescence intensity of solutions containing (i) NMM alone, (ii) NMM+**T**+**P/G4**+Exo III, (iii) NMM+**P/G4**+Exo III, (iv) NMM+metalized **T**+biothiols+**P/G4**+Exo III, (v) NMM+metalized **T**+**P/G4**+Exo III, (vi) NMM+metalized **T**+biothiols-NEM+**P/G4**+Exo III, respectively and bottom shows corresponding photographs taken under a UV transilluminator. Error bars were estimated from at least three independent measurements.

fluorescence measurements were carried out to test the coupling of Exo III with silver deposited DNA for biothiols analysis (Fig. 1d). Samples containing biothiols extracted T displayed about an eight fold increase in the fluorescence, which is similar to that of samples containing **T**. However, in the control experiments where silver metalized **T** was added directly or biothiols were inhibited by N-ethyl-maleimide (NEM), no luminescence changes were observed. Moreover, the fluorescence differences could be obviously distinguished by naked eyes under UV illumination (Fig. 1d). The above results indicated that silver metallization effectively blocked the encapsulated DNAs and the biothiols mediated DNA extraction could be directly subjected to Exo III based amplified sensing platform.

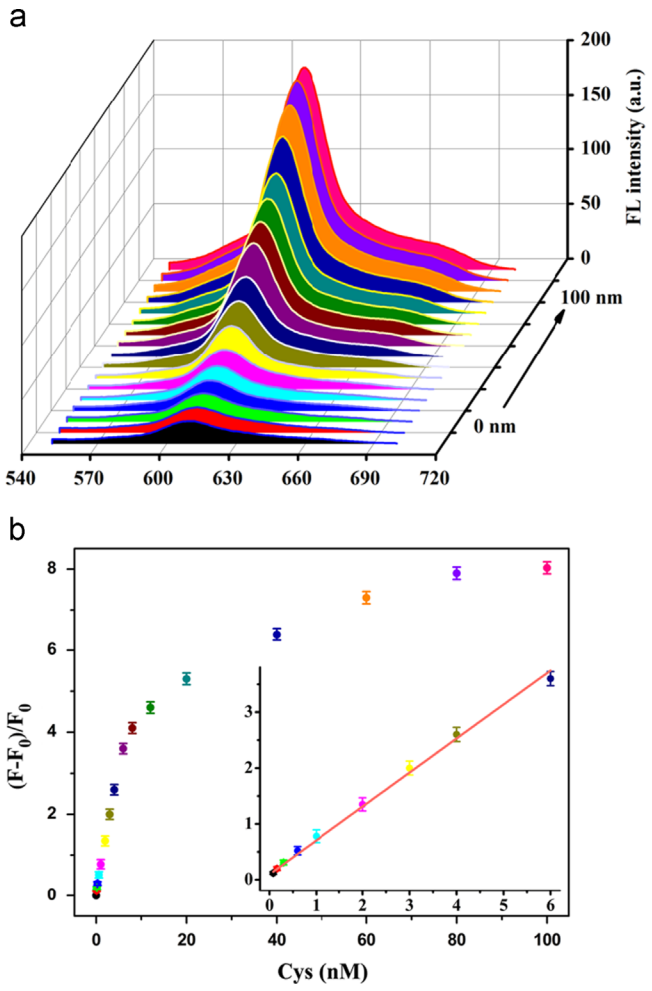

Fig. 2. (a) Fluorescence emission spectra of NMM upon the addition of increasing Cys. (b) Plots of the fluorescence intensity measured at 609 nm as a function of the Cys concentration. Inset: the linear plot. Error bars were estimated from at least three independent measurements.

3.2. Determination of biothiols

To assess the sensitivity of this strategy, quantitative analysis was performed by monitoring the fluorescence of NMM upon incubation with a series of concentrations of biothiols. As shown in Fig. 2a, the fluorescence intensity gradually enhanced upon the addition of increased Cys, thus indicating that the Exo III catalyzed recycle was highly dependent on the concentration of Cys. The fluorescence enhancement at 609 nm ($F-F_0/F_0$) was plotted as a function of Cys concentration. Under the optimal conditions, a linear region was observed between 0–6 nM and the detection limit in our work was estimated to be 7 pM, which was much superior to previous reported methods. In addition, the fluorescence data of Hcy (Fig. S3, in the Supplementary information) and Gsh (Fig. S4, in the Supplementary information) were similar with that of Cys and their detection limits were 8 pM and 5 pM, respectively. The high sensitivity could be attributed to the dual factors: firstly, the specific interactions between NMM and the released G-quadruplex led to significant fluorescence

Table 1
Determination of thiol compounds in human plasma.

Sample	Determined thiol compounds (μM)	Added Cysteine (μM)	Found (μM)	Recovery (%)	RSD ($n=3$, %)
1	318.4	150	476.3	103.2	3.91
		300	614.2	98.2	3.57
2	262.8	150	409.8	99.2	2.85
		300	560.5	99.4	2.62

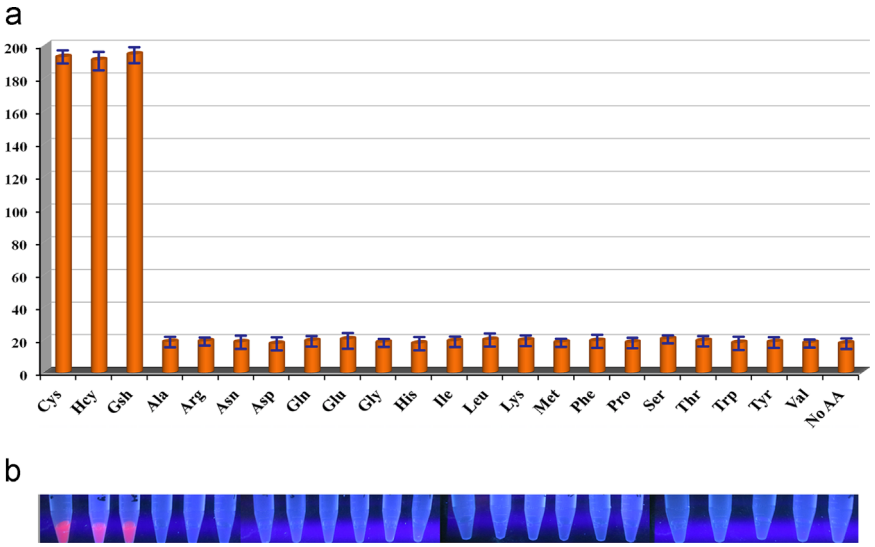

Fig. 3. (a) Fluorescence response of the platform toward biothiols or other essential amino acids. Error bars were estimated from at least three independent measurements. (b) Corresponding photographs of the solutions taken using a UV transilluminator.

enhancement. Secondly, the released target DNA repeatedly hybridized with the DNA probe and the cycle started anew to further enlarge the fluorescence signal. The detection limit of the platform was much lower than the normal concentration of biothiols in human fluids, 50–300 mM of Cys in plasma, 0.1–10 mM of GSH in cell, and 5–15 mM of Hcy in plasma, indicating that the platform may be competent for early detection of disease. In addition, the label-free and turn-on sensing mode offered additional advantages here. Therefore, these results indicated that the platform designed herein could serve as efficient approach for amplified detection of biothioils with ultralow detection limit.

3.3. Selectivity towards biothiols

We further investigated the selectivity of the sensing platform described here by examining the fluorescence responses of the sensor toward other amino acids under the same conditions as the case of biothiols. As shown in Fig. 3a, fluorescence intensity of NMM toward biothiols was much stronger than that toward other 19 amino acids which only induced negligible fluorescence changes. The excellent specificity could be attributed to the intriguing interaction between silver and thiols. Besides fluorescence analysis, the remarkable selectivity toward biothiols over interfering substances can also be observed by the naked eye with aid of a UV transilluminator (Fig. 3b). Obviously, the solutions containing biothiols exhibited red light, while the solutions containing other amino acids exhibited no emission. These observations strongly support the sensing mechanism of our method, and it provides a highly selective and reliable approach for detecting biothiols.

3.4. Samples analysis-determination of biothiols in human serum samples

The excellent specificity combined with high sensitivity to biothiols suggested that our method might be utilized for monitoring biothiols in real samples. Cys was used as the standard during the standard addition analysis (Ros-Lis et al., 2004; Sreejith et al., 2008). As expected, the method had good recoveries and the obtained results were in good agreement with previous reports (Table 1) (Ros-Lis et al., 2004; Sreejith et al., 2008). In control experiments where samples were pretreated with thiol blocking reagent NEM, no significant florescence enhancement was observed (Fig. S5, in the Supplementary information), the results demonstrated that the extraction of DNA was indeed induced by plasma biothiols. These results suggested that our method promises great potential for quantitative analysis of biothiol levels in practical samples.

4. Conclusion

In summary, the present study has introduced the utilization of Exo III biocatalyst and silver metallization of DNA for amplified analysis of biothiols at picomolar concentration. The protocol relies on the amplification process achieved by the recycling of biothiols retrieved target DNA from silver depositions and the specific interactions between quadruplex and its binding ligand. The method has several important features. Firstly, the method reported here is simple in design and economic in operation. Secondly, due to the intriguing interactions between thiol and silver, the method possesses excellent selectivity over other 19 essential amino acids found in proteins, as well as in serum samples. Thirdly, with the aid of an UV transilluminator, the detection and discrimination process could be seen by the naked eye. Therefore, this new concept may offer a potential approach for practical applications as an efficient biosensor for early detection of diseases.

Acknowledgments

Financial support was provided by the National Basic Research Program of China (Grant 2012CB720602, 2011CB936004) and the National Natural Science Foundation of China (Grants 21072182, 21210002, and 91213302)

Appendix A. Supporting information

Supplementary data associated with this article can be found in the online version at http://dx.doi.org/10.1016/j.bios.2014.02.078.

References

Braun, E., Eichen, Y., Sivan, U., Ben-Yoseph, G., 1998. Nature 391, 775–778.
Cho, E.C., Cobley, C.M., Rycenga, M., Xia, Y., 2009. J. Mater. Chem. 19, 6317–6320.
Duan, R., Zuo, X., Wang, S., Quan, X., Chen, D., Chen, Z., Jiang, L., Fan, C., Xia, F., 2013. J. Am. Chem. Soc. 135, 4604–4607.
Freeman, R., Liu, X., Willner, I., 2011. Nano Lett. 11, 4456–4461.
Herzenberg, L.A., De Rosa, S.C., Dubs, J.G., Roederer, M., Anderson, M.T., Ela, S.W., Deresinski, S.C., Herzenberg, L.A., 1997. Proc. Natl. Acad. Sci. U.S.A 94, 1967–1972.
Hignett, G., Threlfell, S., Wain, A.J., Lawrence, N.S., Wilkins, S.J., Davis, J., Compton, R.G., Cardosi, M.F., 2001. Analyst 126, 353–357.
Hu, D., Pu, F., Huang, Z., Ren, J., Qu, X., 2010. Chem. Eur. J. 16, 2605–2610.
Jacobsen, D.W., 1998. Clin. Chem. 44, 1833–1843.
Jin, Z., Sun, W., Ke, Y., Shih, C.-J., Paulus, G.L. C., Hua Wang, Q., Mu, B., Yin, P., Strano, M.S., 2013. Nat. Commun. 4, 1663.
Ju, E., Yang, X., Lin, Y., Pu, F., Ren, J., Qu, X., 2012. Chem. Commun. 48, 11662–11664.
Keren, K., Berman, R.S., Braun, E., 2004. Nano Lett. 4, 323–326.
Keren, K., Krueger, M., Gilad, R., Ben-Yoseph, G., Sivan, U., Braun, E., 2002. Science 297, 72–75.
Lee, J.-S., Ulmann, P.A., Han, M.S., Mirkin, C.A., 2008. Nano Lett. 8, 529–533.
Lin, Y., Tao, Y., Pu, F., Ren, J., Qu, X., 2011. Adv. Funct. Mater. 21, 4565–4572.
Liu, J., Lu, Y., 2003. J. Am. Chem. Soc. 125, 6642–6643.
Liu, J., Lu, Y., 2007. Angew. Chem., Int. Ed. 46, 7587–7590.
Liu, X., Freeman, R., Willner, I., 2012. Chem. Eur. J. 18, 2207–2211.
Lu, C., Zu, Y., Yam, V.W. W., 2007. J. Chromatogr. A 1163, 328–332.
Ma, D.L., He, H.Z., Leung, K.H., Zhong, H.J., Chan, D.S. H., Leung, C.H., 2013. Chem. Soc. Rev. 42, 3427–3440.
Peng, L., Zhu, Z., Chen, Y., Han, D., Tan, W., 2012. Biosens. Bioelectron. 35, 475–478.
Quaroni, L., Chumanov, G., 1999. J. Am. Chem. Soc. 121, 10642–10643.
Ros-Lis, J.V., García, B., Jiménez, D., Martínez-Máñez, R., Sancenón, F., Soto, J., Gonzalvo, F., Valldecabres, M.C., 2004. J. Am. Chem. Soc. 126, 4064–4065.
Song, S., Qin, Y., He, Y., Huang, Q., Fan, C., Chen, H.-Y., 2010. Chem. Soc. Rev. 39, 4234–4243.
Sreejith, S., Divya, K.P., Ajayaghosh, A., 2008. Angew. Chem., Int. Ed. 47, 7883–7887.
Stryer, L., 1995. Biochemistry, 4th ed. W.H. Freeman, Company, New York p. 21
Tanaka, F., Mase, N., Barbas Iii, C.F., 2004. Chem. Commun., 1762–1763
Tcherkas, Y.V., Denisenko, A.D., 2001. J. Chromatogr. A 913, 309–313.
Wang, L., Liu, X., Hu, X., Song, S., Fan, C., 2006. Chem. Commun., 3780–3782
Wei, X., Lin, W., Ma, N., Luo, F., Lin, Z., Guo, L., Qiu, B., Chen, G., 2012. Chem. Commun. 48, 6184–6186.
Wulfkuhle, J.D., Liotta, L.A., Petricoin, E.F., 2003. Nat. Rev. Cancer 3, 267–275.
Xiao, Y., Lubin, A.A., Heeger, A.J., Plaxco, K.W., 2005. Angew. Chem. 117, 5592–5595.
Yi, L., Li, H., Sun, L., Liu, L., Zhang, C., Xi, Z., 2009. Angew. Chem., Int. Ed. 48, 4034–4037.
Zen, J.-M., Kumar, A.S., Chen, J.-C., 2001. Anal. Chem. 73, 1169–1175.
Zhang, M., Yu, M., Li, F., Zhu, M., Li, M., Gao, Y., Li, L., Liu, Z., Zhang, J., Zhang, D., Yi, T., Huang, C., 2007. J. Am. Chem. Soc. 129, 10322–10323.
Zhao, C., Wu, L., Ren, J., Qu, X., 2011. Chem. Commun. 47, 5461–5463.
Zhao, X., Tapec-Dytioco, R., Tan, W., 2003. J. Am. Chem. Soc. 125, 11474–11475.
Zuo, X., Xia, F., Xiao, Y., Plaxco, K.W., 2010. J. Am. Chem. Soc. 132, 1816–1818.